

# Development of Chitosan-Based Nanoemulsion Gel Containing Microbial Secondary Metabolite with Effective Antifungal Activity: In vitro and in vivo Characterizations

Muhammad Khalid Khan<sup>1</sup>  
Barkat Ali Khan<sup>1</sup>  
Bushra Uzair<sup>2</sup>  
Shah Iram Niaz<sup>3</sup>  
Haroon Khan<sup>4</sup>  
Khaled Mohamed Hosny<sup>5</sup>  
Farid Mena<sup>6</sup>

<sup>1</sup>Drug Delivery and Cosmetics Laboratory (DDCL), Faculty of Pharmacy, Gomal University, Dera Ismail Khan, 29050, Pakistan; <sup>2</sup>Department of Biotechnology and Bioinformatics, International Islamic University, Islamabad, 40000, Pakistan; <sup>3</sup>Department of Chemistry, Institute of Chemical Sciences, Gomal University, Dera Ismail Khan, 29050, Pakistan; <sup>4</sup>Department of Pharmaceutical Chemistry, Faculty of Pharmacy, Gomal University, Dera Ismail Khan, 29050, Pakistan; <sup>5</sup>Department of Pharmaceutics, Faculty of Pharmacy, King Abdulaziz University, Jeddah, 21589, Saudi Arabia; <sup>6</sup>Department of Nanomedicine, California Innovations Corporation, San Diego, CA, 92037, USA

**Purpose:** Microbial resistance to antibiotics is one of the most important public health concerns of the 21<sup>st</sup> century. We isolated, purified, and structurally elucidated antifungal secondary metabolites from red soil microbes and encapsulated them into chitosan (CS)-based nanoemulsion (NE) gel (NEG).

**Methods:** Three compounds were isolated and purified of which only one compound (Pure 2) showed potent antifungal activity (MFC: 8–132 µg/mL), which was also significantly ( $P < 0.05$ ) more efficient than fluconazole (MFC: 32–132 µg/mL). Pure 2 was structurally elucidated using 1D- and 2D-NMR before its incorporation into NEG. The formulations were prepared by high-speed homogenization technique. Physicochemical and pharmacological characterizations of formulations (ie, droplet size, PDI, zeta potential, drug content, viscosity, SEM, FTIR, spreadability, in vitro drug release, ex vivo permeation, in vitro antifungal and in vivo antifungal activities) were assessed.

**Results:** NMR analyses identified the compound as a derivative of phthalic acid ester (PAE). The optimized formulations displayed a droplet size  $< 100$  nm, -ve zeta potential, and PDI  $< 0.45$ . The drug content was within the official limit of pharmacopeia (ie,  $100 \pm 10\%$ ). Insignificant changes ( $P > 0.05$ ) in the viscosity of the formulations stored were observed. The morphology of the formulations indicated mesh-like structure. The FTIR study indicated that there were no interactions between the drug and other ingredients of the formulations. Optimum spreadability was observed in all formulations. NEG released  $75.3 \pm 1.12\%$  of Pure 2 after 12 hrs while NE released  $85.33 \pm 1.88\%$  of the compound. The skin permeation of F2 ( $71.15 \pm 1.28\%$ ) was significantly different ( $P < 0.05$ ) from F3 ( $81.80 \pm 1.91\%$ ) in rabbits. Complete and apparently safe recovery from the fungal infection was achieved in rabbits treated topically with Pure 2-loaded NEG.

**Conclusion:** Hence, the NEG-loaded PAE isolated from *Pseudomonas fluorescens* represents a possible alternative for the treatment of fungal infections as compared to available therapies.

**Keywords:** fungal resistance, red soil, *Pseudomonas fluorescens*, microbial secondary metabolites, phthalic acid ester derivative, nanoemulsion gel

## Introduction

Fungal infection of skin is a common dermatological problem that presents a challenging dilemma for clinicians throughout the world.<sup>1</sup> The frequency of susceptibility and sensitivity to various fungal infections has increased significantly

Correspondence: Muhammad Khalid Khan  
Email khalid.gomalian@gmail.com



which has caused high morbidity and mortality since early 1980s.<sup>2</sup> The occurrence of superficial fungal infections of skin hairs and nails among different mycotic infections has increased in the last century.<sup>3</sup> More than 20–25% of the world population has been infected with different fungal infections.<sup>4</sup> It is estimated that globally more than 500 million people are infected and each year two million people are killed by these fungal infections in both under-developed and developed countries.<sup>5</sup>

The most prevalent type of superficial infection in human is cutaneous candidiasis caused by different species of *Candida*, targeting immune-compromised individuals. The treatment of candidiasis is limited to a small number of antifungal agents, mainly azoles derivatives, but due to the increased toxicity issues and azole resistance their application is limited.<sup>6</sup> Besides, infections caused by *Aspergillus* species have also increased during the recent years and are considered through the CDC's 2019 report (CDC's watch list) as a serious threat to humans. These infections have achieved a mortality ratio higher than 80% and exceeded the frequency and prevalence of candidiasis.<sup>7</sup> Globally, among all *Aspergillus* species, the most common is *A. fumigatus* accounting for 85–90% of all *Aspergillus* infections.<sup>8</sup>

Microbial resistance to antibiotics is one of the most important public health concerns of the 21<sup>st</sup> century and a big concern for the treatment and management of several infections caused by pathogenic microbes.<sup>9,10</sup> The development of infections at a fast pace and multidrug resistance (MDR) have prompted the search for bioactive metabolites with broad-spectrum antimicrobial activities from natural sources including plants and microbes, as well as original formulations of antibiotics and novel antibiotics having modified chemical structures and ability to target new sites.<sup>10</sup>

Topically applied transdermal formulations have numerous advantages including site targeting,<sup>11</sup> minimizing side effects associated with oral preparations,<sup>12</sup> high patient acceptance, enhanced patient compliance, and improved therapeutic efficacy.<sup>13</sup> The topical formulations show their efficacy if the drug from these formulations releases and penetrates the layers of skin, which will create an effective drug depot.<sup>12</sup> However, there are some limitations in therapeutic efficacy of several drugs. These may be due to impaired physicochemical properties of the drug substances and dosage forms. The conventional available dosage forms like ointments, gels, and creams have their own limitations,

including a larger particle size of drug substances. The physiological availability of the drug at the site of action is dependent on the particle size of the drug.<sup>13</sup>

Nanoemulsions are thermodynamically stable drug delivery systems having extremely small droplet size in the range of 100–1000 nm. These are colloidal dispersions having two immiscible liquids which are stabilized by the addition of surfactants or co-surfactants.<sup>12,13</sup> Nanoemulsions help to enhance the bioavailability and onset of action of drugs by improving solubility and dissolution. They have the ability to deliver both hydrophilic and hydrophobic drugs as well as to achieve sustained drug release.<sup>13</sup> However, in spite of several advantages, nanoemulsions are limited by their low viscosity, which remains a challenge for their transdermal application. To overcome this problem, various suitable gelling agents including polymers and copolymers are used to enhance the viscosity of the nanoemulsions and in turn improve the therapeutic efficacy.<sup>14</sup>

Gels are widely accepted for dermatological application as they possess several favorable properties that include being emollient, non-staining, and easily removable, optimum spreadability, non-greasiness, higher compatibility with several other excipients, water-soluble and pseudo-plastic.<sup>12</sup> Gels can be incorporated into nanoemulsion leading towards the formation of nanoemulgel or nanoemulsion gel. The polymers in gels form a three-dimensional hydrogel network which entrap nanoemulsions globules.<sup>12,13,15</sup>

Nanoemulsion gels are of the nanoemulsion of oil in water (O/W) or water in oil (W/O) type which are gelled by the addition or incorporation of suitable gelling agents. They possess the features of both nanoemulsion and gels, and therefore they have higher patient acceptability.<sup>15</sup>

This study aimed to (i) isolate, purify, and identify novel natural-sourced antifungal agents, and (ii) formulate the best antifungal compound in CS-based NEGs.

## Materials and Methods

### Chemicals

Peptone, glycerol, MgSO<sub>4</sub>, K<sub>2</sub>PO<sub>4</sub> (as King's B media), nutrient agar, nutrient broth, and PDA (Oxoid, UK) were used. Ethanol (Merck, Germany) and ethyl acetate (Sigma, France) was used as solvent, while n-hexane, methanol, chloroform, dichloromethane, and acetone (Sigma Aldrich, Germany) were used for fractionations. Thin-layer chromatography (TLC) cards were used to check purification

of compounds. Silica gel (Marine Chemical Inc, China) and Sephadex (LH-20 green herbs, Beijing, PRC) were used for purification of various compounds from microbial extract. Tween 80 was used as a surfactant, PEG 400 as co-surfactant, cetostearyl alcohol as a preservative, CS as a gelling agent, and eucalyptus oil as oil phase. Distilled water (D/W) was used for the preparations of any solutions.

## Isolation and Identification of Microbial Strains from Red Clay

For isolation of microbial strains, a soil sample was collected from the District Karak region of Khyber Pakhtunkhwa, Pakistan and transferred to the laboratory in sterile polyethylene bags. The sample was serially diluted with 1% peptone. The soil extract was autoclaved and spread on nutrient agar and King's B selective growth media and incubated at 37°C for 24 hrs. The isolated bacterial colonies were identified based on their colonial and cellular morphology as well as biochemical features.

The colony characteristics (size, shape, color) were examined on solid media, cellular morphology was examined through microscopy, and biochemical identification was assessed through API NE 20 kit and Gram staining.<sup>1</sup>

## Preparation of the Microbial Crude Extract

*P. fluorescens*, identified and obtained from bacterial cultures of red soil, was selected after secondary screening for the extraction of bioactive compounds (secondary metabolites) by the method of solid-state fermentation.<sup>1,2</sup> For this purpose, King's B agar (2000 mL) plates with 35% glycerol were made, and *fluorescens* was inoculated before the plates were incubated at 37°C. Similarly, the *fluorescens* was also grown in King's B broth media in 1000 mL bottles containing 30% glycerol. After one week, the culture medium from all the plates and bottles was transferred into 1000 mL beakers and flasks and chopped into small pieces using a cutter and stirrer rod, and 10 g of NaCl was added. Acetone (80%) was prepared and added to the flasks containing the crumbled media and allowed for 40 min. The secondary metabolites were separated from the solid residue by filtering the acetone and fermented mixture using a cotton cheese cloth. After this, ethyl acetate was added and the flasks shaken vigorously. This mixture was transferred into the separating funnels having capacity of 1000 mL. The funnels were allowed to stand for 1

h until two visible layers appeared. The lower layer was discarded, and the upper organic layer was taken in a beaker. Using a rotary evaporator (Rotavapor, Buchi 410, Germany), the organic solvent was evaporated, and dried residues were obtained. The resulting metabolites were kept at 4°C for further analysis.<sup>1</sup>

## Isolation and Purification of the Secondary Metabolites

For the isolation and purification of compounds from the *fluorescens* crude extract, a medium size column was selected, and silica having mesh size 230–400 was loaded. The dried slurry was incorporated into the column, and solvents having different polarities were passed over it. A gradient of n-hexane and methanol was used, and fractions were eluted. The fractions were collected and dried in a rotary evaporator and confirmed by TLC cards. The TLC cards were dried and visualized under the UV at 254 nm and 366 nm using a spectrophotometer. Those fractions were combined that showed the presence of pure compound based on TLC profile. To remove any minor impurities from the compounds, the purified combined fractions were reloaded in silica and Sephadex column.<sup>15</sup> The eluted n-hexane:methanol (80:20) fraction showed the presence of a single UV active compound. Three compounds were purified using the same procedure but with different ratios of solvents.<sup>16–18</sup> These compounds were then named as Pure 1, Pure 2, and Pure 3.

## Minimum Fungicidal/Fungistatic Concentration of Purified Compounds

The minimum fungicidal/fungistatic concentration (MFC) of each purified compound was determined by microtiter broth dilution, as explained in Clinical and Laboratory Standard Institution.

## In vitro Antifungal Activity of Purified Compound

The purified compound (Pure 2) that showed the best MFC was selected for in vitro antifungal activity. Antifungal activity of the Pure 2 compound was determined by Kirby–Bauer disc diffusion method according to the previous studies.<sup>1,2</sup> DMSO was used as a control. Fungal strains including *Trichophyton tonsurans*, *Candida albicans*, *Aspergillus niger*, *Aspergillus fumigatus*, and *Saccharomyces cerevisiae* were spread over the nutrient agar and Muller–Hinton agar plates using sterile swabs.

**Table 1** Composition of Nanoemulsions (NE) with Varying Concentrations of Ingredients

Formulations Codes	Eucalyptus Oil (w/w)	PEG-400 (w/w)	Polysorbate-80 (w/w)	Drug (w/w)	Distilled Water Q.S. to 100 g
NE-1	15 g	20 g	15 g	-	50.00 g
NE-2	20 g	15 g	14 g	500 mg	50.50 g
NE-3	17 g	18 g	12 g	500 mg	52.50 g
NE-4	20 g	15 g	10 g	500 mg	54.50 g

**Note:** NE, blank nanoemulsion.

A sterile filter paper disc of about 6 mm containing 100–150  $\mu$ L of purified compound dissolved in DMSO was placed on the agar plates. These plates were then placed in an incubator (BIOBASE, China) at 37°C $\pm$ 2. After 48 hrs, the zones of inhibition (ZIs) were calculated and recorded in mm. All the values were calculated in triplicate, and results were averaged.

## Structure Elucidation by NMR Spectroscopy

The Pure 2 compound that showed the best in vitro fungal inhibition (MFC and ZI) was selected for NMR structure elucidation using 1D and 2D NMR according to a protocol previously published.<sup>17</sup> After NMR spectroscopic analysis, the compound was identified as phthalic acid ester (PAE) derivative (NMR data not shown, but available upon request). The structure (<https://pubchem.ncbi.nlm.nih.gov/compound/Phthalate>) and other information about PAE have been recently reviewed.<sup>19–21</sup>

## Preparation of the Nanoemulsion (NE)

NE was prepared by high-pressure homogenization technique according to a previously published method<sup>15,19</sup> slightly modified. The oil phase (A) of NE was prepared by mixing eucalyptus oil with PEG-400 and the compound/drug (Pure 2). The aqueous phase (B) was prepared by adding Tween-80 to D/W. Both the phases (A +B) were kept in water bath (Precision Scientific, Model 181, Japan) at 50°C $\pm$ 5 for 30 min. After heating both phases, the oil phase was added dropwise to the aqueous phase under stirring (1500 rpm) for 10 min. The formulation was gradually cooled, and the speed of the stirrer was reduced to 1000 rpm for 10 min. For proper mixing, the speed of the stirrer was again increased up to 1500 rpm for 10 min until a uniform emulsion was obtained. The emulsion was allowed to cool and

subjected to high-speed/high-shear homogenizer (Daihan, Korea) at 15,000 rpm for 10 min. For optimization, different formulations (varying in concentration of ingredients) were prepared (Table 1).

## Stability of Nanoemulsions

NE formulations were inspected organolaptically before mixing them with CS gelling solution. For this purpose, their color change, consistency, and phase separation were observed. To assess their thermo-stability and capacity to be stored, samples of each formulation were kept at different temperatures (8°C, 25°C, 40°C, and 40°C+75, relative humidity (RH)) for 28 days.<sup>19</sup>

## Preparation of CS Gelling Solution

The chitosan gel was prepared by dispersing 2 g of CS in 100 mL D/W containing 2% acetic acid.<sup>15</sup> The gel prepared was kept overnight before incorporating into NE formulations.

## Preparation of Nanoemulsion Gel (NEG)

NE was mixed with CS gelling solution at 1:1 ratio and under constant gentle stirring for at least 15 min. A uniform semisolid NEG formulation was obtained. The pH of the formulation was adjusted 4.5 to 5.5 as pH of the human skin to avoid any irritation using triethanolamine (TEA).<sup>19</sup>

## Physicochemical Characterizations of NEs and NEG

### Thermodynamic Stability

To test the formulations under stress conditions, the optimized NE and NEG formulations were subjected to thermodynamic stabilities (heat cooling cycle, freeze-thaw cycle, and centrifugation) according to the ICH guidelines and previously published study.<sup>19</sup>

## pH Analysis

All the freshly prepared NE and NEG formulations were subjected to pH analysis, and then evaluated after 12 hrs, 24 hrs, 7 days, and 28 days.

## Droplet Size, Surface Charge, and PDI Measurements

This test was performed to find out the droplet size, surface charge, and polydispersity index (PDI) of NE and NEG formulations. For this purpose, zeta sizer and helium-neon (He-Ne) laser (Nano ZS 90, Malvern Instruments, UK) were used. Accurately 1 mL of NE was diluted with 9 mL of deionized water and mixed thoroughly for 3 min. This procedure was repeated thrice, and the results were averaged.<sup>21</sup>

## Drug Content Analysis

Drug content analysis was carried out according to the method of Burki et al with slight modifications.<sup>19</sup> For this purpose, 1 g of the nanoemulsion was weighed and mixed with 9 mL of ethanol (w/v). This mixture was subjected to centrifugation at 5000 rpm for 2 min using centrifugation (SCIOLOGEX, USA). It was filtered using a nylon filter membrane having a pore size of 0.45  $\mu\text{m}$ . The sample filtrate was analyzed thrice on HPLC (SHIMADZU Nexera-UHPLC 3.0, Japan), and the results were averaged.

## Viscosity Evaluation

The viscosities of the selected NE and NEG formulations were evaluated using a viscometer (NDJ, 8S, Korea) at 8°C, 25°C, and 40°C on days 0, 1, 2, 7, 14, and 28.

## FTIR Measurements

The selected compound, CS powder, NE, and NEG formulations were subjected to FTIR spectroscopy (Perkin, Elmer, United Kingdom) to determine the compatibility between the polymer and constituents of the formulations. Samples of each ingredient and formulations were kept on the diamond crystal and pressed by the knob. The spectrum of each sample was recorded in triplicate in the wavenumber range of 400–4000  $\text{cm}^{-1}$ .<sup>15</sup>

## Morphological Pictures

The shape of the nanoemulsion formulations were examined using SEM (Quanta FEG, UK). Samples of formulations were applied on the metal stubs using double-sided adhesive tape. The formulation-loaded stubs were kept in a vacuum chamber for drying. Before observation, the samples were coated for 5 min with gold having 10 nm thickness with the help of a sputter coater. The stubs were examined in SEM at

accelerating voltage of 10 kV and magnification of 10,000 $\times$ . The specific sections of the samples were photographed according to the reported methods.<sup>23,24</sup>

## Spreadability of NEG

The spreadability of the prepared formulations was determined by a “Drag and Slip” apparatus. This apparatus is simply made of a wooden block connected to a pulley from one end. It consists of two glass slides of the same dimensions, of which one is fixed on the block and the other is movable. The sample is then sandwiched between the stationary slide and the upper movable slide, and a measured weight is placed on it. Accurately weighed 2 g of the optimized formulations was placed on the fixed (stationary) slide and sandwiched by the upper slide. A weight of 50 g was placed on the upper glass slide. The time taken by the upper slide to cover a distance of 8 cm was noted. Using the following equations, the spreadability of the test NEG was calculated.

$$S = M \times L \div T \quad (\text{Eq.1})$$

Where S indicates spreadability, M is the weight placed on the upper glass slide, L indicates length of glass slides, and T is the time taken by the slides to cover the distance.

## In vitro Drug Release

The in vitro drug release study was performed according to the previous study conducted by Khan et al.<sup>11</sup> Franz diffusion cell (IPS Technologies, India) was used for this purpose and consists of receptor and donor compartments having capacity of 6 mL and 3 mL, respectively. Prior to loading NE and NEG samples, the temperature was maintained at 37°C $\pm$ 1°C under stirring (300 rpm). A tuffryn membrane (Sortorius, Germany) was clamped between the receptor and donor compartments. The receptor compartments were filled with sodium acetate buffer having 5.5 pH, and 2 g of each formulation was loaded on the donor compartment. At specific time intervals (ie, 0 h, 1 h, 2 hrs, 4 hrs, 8 hrs, and 12 hrs), the sample (2 mL) was collected from the receptor compartment using a spinal syringe. To maintain the sink condition in the receptor compartment, a fresh buffer was introduced. The samples collected were then analyzed by HPLC (PerkinElmer LC 300, Richmond, Ca, USA).

## Ex vivo Study

### Ethics

This study was approved by the Ethical Review Board (ERB) of Gomal University, D.I. Khan, Pakistan, under

the reference #851/QEC/GU. All the experiments were performed according to the NIH guidelines.

## Preparation of Rabbit Skin and Permeation Study

The rabbit skin was prepared for ex vivo permeation analysis according to the study of Burki et al.<sup>19</sup> A male rabbit (approx. 1.5 kg) was purchased from the local market of the District D.I. Khan, Pakistan. Using vanishing cream, hairs from the dorsal skin of the rabbit were removed. The rabbit was then sacrificed by cervical dislocation, a commonly used method for <2.2 lb rabbit euthanasia. The skin was excised using a surgical blade and washed, defatted, and, prior to storage in the refrigerator, it was covered in aluminum foil for further use. On experiment day, it was soaked in warm water for 1 h before clamping in the Franz diffusion cell for ex vivo permeation.

The ex vivo drug permeation study was performed according to a previous study.<sup>19</sup> The skin, which was previously prepared for this purpose, was clamped between the receptor and donor compartments. The receptor compartments of two cells were filled with phosphate buffer solution (1× PBS, pH 7.4), and 2 g of each formulated sample was loaded on the donor compartment. At specific time intervals (ie, 1 h, 2 hrs, 4 hrs, 8 hrs, 16 hrs, and 24 hrs), the samples (2 mL) were then collected and analyzed by HPLC (PerkinElmer LC 300, Richmond, CA, USA).

## Antifungal Activities of the Nanoemulsions

### In vitro Antifungal Assays

In vitro antifungal assays of the drug-loaded nanoemulsions were performed according to a previous protocol slightly modified.<sup>1,2</sup> Test microorganisms included *Candida albicans*, *Aspergillus niger*, *Trichophyton tonsurans*, and *Aspergillus flavis*. Agar media were prepared by dissolving 2 g of nutrient agar (Himedia, India) in 100 mL of distilled water. This solution was autoclaved at 125°C and 15 PSI for 1 h. The fungal strains were spread over the agar plates with the help of sterile swabs, and, with a borer, a hole was punched in the middle of all the agar plates before 100 µL of each drug-loaded nanoemulsion was introduced to it. The plates were covered and kept in an incubator (BIOBASE, China) at 37°C±1°C for 48 hrs.

The zones of inhibition (ZIs) of NEG against each fungal strains were measured using a digital Vernier caliper.

### In vivo Antifungal Assays

To evaluate the in vivo antifungal activity of prepared nano-formulations, male rabbits ( $N=12$ ) were purchased and divided into three groups ( $n=4$ ). The rabbits were assigned to control group (Group 1/blank NEG), standard group (Group 2/marketed antifungal agent Canesten<sup>®</sup>), and experimental group (Group 3/compound-loaded NEG). Each group of rabbits was kept in separate cages with standard diet, at the animal house at Gomal Centre of Pharmaceutical Sciences, Faculty of Pharmacy, Gomal University, D.I. Khan, Pakistan.

*Candida albicans*, as an infectious agent, was used to induce infection in all the studied rabbits. The organism was obtained from Laboratory of Microbiology, Department of Biotechnology, International Islamic University (IIU), Islamabad, Pakistan. The obtained fungal species were maintained on nutrient agar plates and kept in a refrigerator at 4°C. The organisms were freshly cultured to revive before applying on the animals. The dorsal area of each rabbit was depilated. The fresh cultured infectious inoculum of *C. albicans* was applied on the depilated surface of rabbits and left for 3 days, the time required to get the first symptoms (ie, redness and scales) of active infection. The treatment was started on day 4, and each formulation was applied to the animals in once a day (OD) frequency. The treatment was continued until complete recovery from infection (12 days). The antifungal activity of each formulation was evaluated daily by macroscopic examination of the infected area.

### Statistical Analysis

One-way ANOVA and Student's *t* test were applied to the data using IBM SPSS version 20. All the values obtained from three independent experiments were averaged and presented as mean±SD.

## Results and Discussion

### Isolation and Identification of *Pseudomonas fluorescens*

In the preliminary screening, only one bacterial strain (out of 15 tested), isolated from red soil samples, had the capability to inhibit the growth of different fungi (ie, *Trichophyton tonsurans*, *Trichophyton rubrum*, *Candida albicans*, *Aspergillus niger*, *Aspergillus fumigatus*, *Saccharomyces cerevisiae*). Based on the colonial and

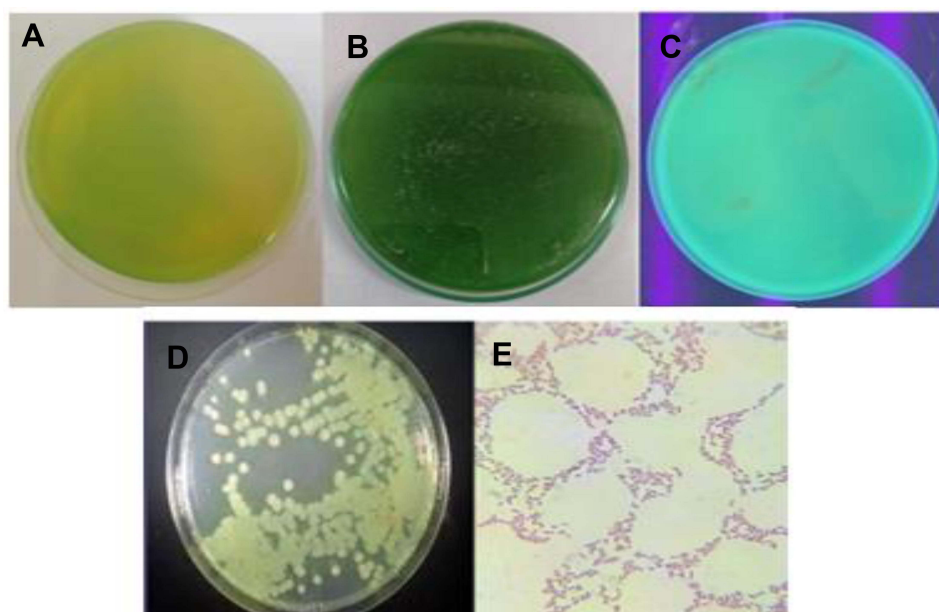


**Figure 1** Colony morphology of *Pseudomonas fluorescens*, after 24 hrs growth on (A) nutrient agar plate, (B) King's B medium plate, (C) under UV-visible light, (D) streak culture on nutrient agar plate, and (E) microscopic image (100×) on nutrient agar plate.

cellular morphology, the bacterial strain was characterized (Figure 1). The isolate appeared as Gram -ve rods upon staining. It displayed smooth, spherical, and medium size, under a 100× microscope lens. After 24 hrs of incubation either on nutrient agar plate (Figure 1A) or King's B medium plate (Figure 1B), a yellow-green pigment produced by the isolate was observed, which was hypothesized as *Pseudomonas fluorescens*. The isolate was further observed under UV light (Figure 1C), where the green fluorescence due to the presence of pyoverdine (fluorescein, a siderophore) further strengthened the identification of the strain. The strain formed greenish, large, opaque, flat colonies with irregular margins, and distinctively fruity odor, on nutrient agar plates (Figure 1D). Zoom microscopic viewing of the strain revealed red rod-shaped cellular morphology (Figure 1E). The data from biochemical tests (Voges Proskauer -, indole -, methyl red-, nitrate -, catalase +, oxidase +) definitively confirmed the strain as *fluorescens*. Several studies have reported the colonial morphology and biochemical features of *fluorescens*.<sup>1,2,26</sup>

*P. fluorescens* is generally considered a non-pathogen bacterial species, at least under normal circumstances. Interestingly, this bacterium grows and persists in our bodies and out-compete pathogenic bacteria for space and nutrients. Another key characteristic of *fluorescens* is its prevalence in the soil where it has advantageous properties for plant protection (including against fungi) and

growth.<sup>27</sup> Thus, it was worth investigating this strain for secondary metabolites exerting anti-fungal activity.

## Purification and in vitro Biological Activity of Secondary Metabolites

Three compounds, namely Pure 1, Pure 2, and Pure 3, were purified from the dried slurry of crude extract of *fluorescens* by silica gel and Sephadex using a gradient of n-hexane and methanol at various ratios. The purity of the compounds was verified several times by TLC cards. Compounds having the same TLC were combined (data not shown).

The MFC of the three purified compounds is presented in Table 2. The Pure 2 compound exhibited the best antifungal activity compared to that of Pure 1 and Pure 3 ( $P < 0.05$ ), against the selected fungal strains (ie, *T. tonsurans*, *T. rubrum*, *C. albicans*, *A. niger*, *A. fumigatus*, *S. cerevisiae*). The Pure 1 and Pure 3 did not show any inhibitory actions against these fungal strains. The MFC of the Pure 2 compound ranged from 8 µg/mL to 128 µg/mL against the fungal spores after geometric dilutions in broth, whereas the MFC of fluconazole, used as standard, was found to be 32–128 µg/mL. There was a significant difference ( $P < 0.05$ ) between Pure 2 and fluconazole.

Among the test fungal strains, the *T. rubrum* was extremely sensitive to the purified compound with a ZI of 21.5 mm (Table 3 and Figure 2), followed by *A. niger* (16 mm) > *S. cerevisiae* (14 mm) > *C. albicans* (13 mm) >

**Table 2** MFC of the Purified Compounds and Fluconazole Against Selected Fungal Strains

	Fungal Strains	MFC $\mu\text{g/mL}$			
		Pure 1	Pure 2	Pure 3	Fluconazole
1	<i>C. albicans</i>	–	8	–	32
2	<i>A. fumigatus</i>	–	16	–	64
3	<i>A. niger</i>	–	64	–	128
4	<i>T. rubrum</i>	–	128	–	64
5	<i>S. cerevisiae</i>	–	64	–	128
6	<i>T. tonsurans</i>	–	–	–	128

Note: Dash (–) indicates no activity.

**Table 3** Antifungal Activity of Pure 2 and Fluconazole Against Various Fungal Strains

Test Strains	Zone of Inhibitions	
	Pure 2	Fluconazole
<i>T. rubrum</i>	21.5 mm	18.5 mm
<i>A. fumigatus</i>	11 mm	10.5 mm
<i>C. albicans</i>	13 mm	10.5 mm
<i>A. niger</i>	16 mm	15.0 mm
<i>S. cerevisiae</i>	14 mm	14.0 mm
<i>T. tonsurans</i>	0 mm	6.0 mm

*A. fumigatus* (11 mm) > *T. tonsurans* (0 mm). *T. tonsurans* was resistant to Pure 2. These results are promising when compared to data reported in the previous study performed by Uzair et al, who evaluated the antifungal and

antibacterial properties of other microbial secondary metabolites against several pathogenic fungi and bacteria.<sup>1</sup> The DMSO used as a control did not show any ZI.

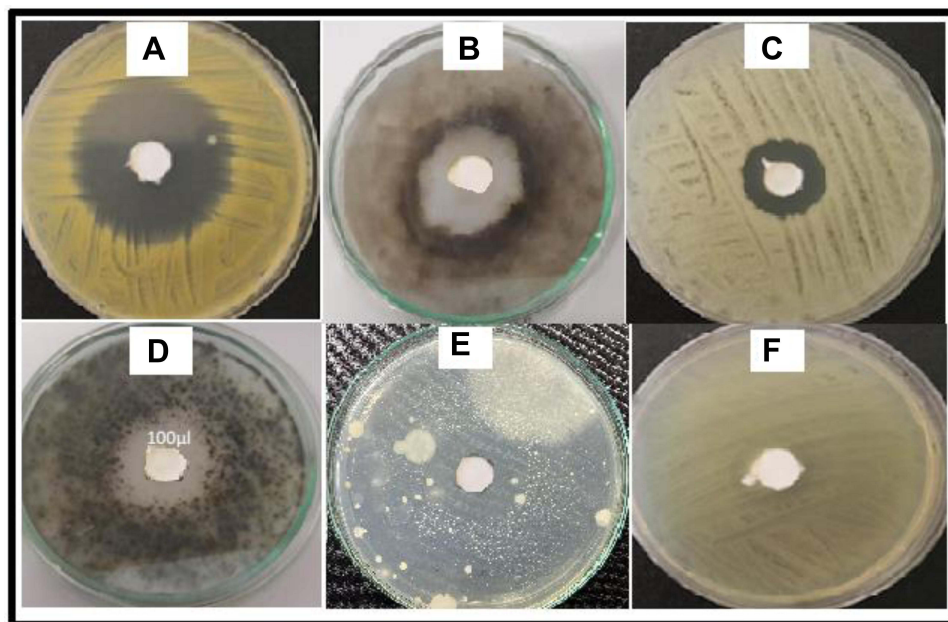
### Identification of Pure 2 as PAE by NMR

The NMR assignment (<sup>1</sup>H, <sup>13</sup>C, DEPT 135, 90, HSQC and HMBC, Data not shown) of the Pure 2 compound was checked on NMR predict (MODGRAPH NMR PREDICT). The compound was identified as phthalic acid bis-2-ethylhexyl ester having the chemical formula C<sub>24</sub>H<sub>38</sub>O<sub>4</sub> and molecular weight of 390.56. It belongs to the group of lipophilic compounds, ie phthalic acid ester (PAE) derivatives which are used in the polymeric materials to enhance their flexibility.<sup>17</sup> It has been reported by many studies that PAE compounds have been found in plants and microorganisms including *Cladophora fracta* (*C. fracta*), *Chaetomorpha basiretorsa* (*C. basiretorsa*), and *Gracilaria lemaneiformis* (*G. lemaneiformis*) and have shown several biological activities like antimicrobial, phytotoxic activity and insecticidal activities.<sup>20,28–30</sup> However, no study has been reported till now on the isolation of PAE from *Pseudomonas* strains nor its antifungal activity in pharmaceutical dosage form.

### Physicochemical Characterizations of the Prepared Nanoemulsions

#### Thermodynamic Stability

The 3 formulations (F1, blank NE; F2, Pure 2-loaded NE; F3, Pure 2-loaded NEG) were kept at different storage

**Figure 2** Antifungal activity of Pure 2 against (A) *T. rubrum*, (B) *A. fumigatus*, (C) *C. albicans*, (D) *A. Niger*, (E) *S. cerevisiae*, and (F) *T. tonsurans*.



conditions (8°C, 25°C, 40°C, and 40°C+75 Relative humidity (RH)) for 28 days and evaluated organolaptically from time to time for phase separation, consistency, liquefaction, color change, and cracking. The freshly prepared nano-formulations were yellowish in color, smooth and without phase separation after centrifugations operated at 5000 rpm and 10,000 rpm.

The nano-formulations were also evaluated at the pH of human skin (ie, 5.5)<sup>15,19</sup> at different time intervals (ie, 12 hrs, 24 hrs, 7 days, 14 days, and 28 days). Statistical analysis by Student's *t* test showed insignificant change ( $P>0.05$ ) in pH in all formulations. The pH is an important factor, as it must range between 5 and 6 for suitable topical application of drugs and to avoid skin irritations.<sup>20–22</sup>

### Droplet Size, PDI, and Surface Charge

The results of droplet size, PDI, and surface charge of the blank NE (F1), Pure 2-loaded NE (F2), and Pure 2-loaded NEG (F3) are presented in Table 4, and Figures S1A–C) and S2A–C), respectively (in the Supplementary materials).

Droplet size has an important role in the formulations used for topical or transdermal delivery of drugs.<sup>15</sup> Several promising parameters like drug release, drug permeation, and biodistribution are affected by the droplet size and the particle size distribution (PSD).<sup>29</sup> F1 has droplet size of  $55.87\pm 0.2$  nm which was significantly the lowest compared to that of F2 and F3. The droplet size of the F2 has increased after loading of drug ( $70.84\pm 0.3$  nm). Our data agree with Sari et al who reported that addition of curcumin to a blank NE formulation increased the droplet size from  $78.7\pm 0.4$  nm to  $83.6\pm 0.7$  nm.<sup>29</sup> Indeed, drug loading affects the size of droplet in the formulation.<sup>25</sup> Similarly, the mean droplet size of F3 was  $80.75\pm 0.9$  nm. Although a small increment in the mean droplet size of F3 was found, compared to F2, the addition of the gelling agent CS to F2 did not significantly increase the droplet size of F2. This result is supported by Eid et al who reported similar findings after addition of Carbopol 940 (as gelling agent) to NE, explained by the enhancement of gelling agent-induced viscosity.<sup>24</sup>

PDI indicates the uniformity and homogeneity of droplet size or size distribution in the formulations. The higher the PDI, the lower will be the uniformity of droplet size/size distribution in the formulation.<sup>24,25</sup> The formulation having a PDI less than 0.45 is considered a homogeneous dispersion. The PDI values of F1, F2, and F3 formulations were 0.135, 0.120, and 0.34,

respectively, indicating the uniformity of droplet size within each formulation.

The surface charge (ZP) of F1 and F2 was negative (ie,  $-23.3$  mV and  $-20.3$  mV, respectively) on their surfaces, whereas ZP of F3 was positive ( $+27.9$  mV) due to addition of CS to F2 because CS is a highly positively charged polymer.<sup>25</sup> The negative ZP is beneficial for enhanced stability of the formulations, while positive ZP can be helpful for efficient topical application of nanoemulsions because the cell membrane is charged negatively, thereby avoiding electrostatic repulsion.<sup>24,32</sup>

### Identification of Functional Groups by FTIR

The ATR-FTIR spectra of Pure 2 (PAE) as a novel anti-fungal compound, blank NE (eucalyptus oil based), pure CS, and NEG (CS-based NE) are provided in Figure 3.

The FTIR spectrum of Pure 2 (Figure 3A) showed the highest peaks at  $3122\text{ cm}^{-1}$  and  $2868.4\text{ cm}^{-1}$ , which are attributed to O–H stretch and C–H stretch vibrations of phenols, respectively. C–H band indicates the possible presence of carboxylic acids, amines, and alkanes. FTIR spectral bands at  $1791\text{ cm}^{-1}$ ,  $1619.5\text{ cm}^{-1}$ ,  $1500.08\text{ cm}^{-1}$ , and  $1286.13\text{ cm}^{-1}$  are assigned to C=O stretch,  $\text{C}=\text{C}$  stretch, N–H bend, O–H, respectively. The sharp peak at  $1113.65\text{ cm}^{-1}$  indicates the presence of aliphatic amines (C–N stretch). These data are in line with other studies which confirmed the presence of large amounts of phenols, carboxylic acids (COOH), alkanes, amines (NH<sub>2</sub>), and aliphatic amine (C–N) compounds in antifungal drugs.<sup>33</sup>

The FTIR spectrum of the NE (Figure 3B) showed characteristic weak bands at  $1090.48\text{ cm}^{-1}$  and  $1460\text{ cm}^{-1}$  attributed to C–O–C symmetrical and C–H<sub>3</sub> symmetrical deformation modes, respectively. These peaks confirmed the presence of 1,8-cineole, the active component in eucalyptus responsible for therapeutic activity of NE.<sup>34</sup> The peaks at  $2920.86\text{ cm}^{-1}$  and  $3429.60\text{ cm}^{-1}$  correspond to the methylene group and OH/NH stretching vibrations, respectively.

The FTIR spectrum of the pure CS (Figure 3C) showed a main peak at  $3389.83\text{ cm}^{-1}$  which is most likely due to OH/NH stretching vibration, and weaker bands observed at  $2929\text{ cm}^{-1}$ ,  $1642.39\text{ cm}^{-1}$ , and  $1085.8\text{ cm}^{-1}$  corresponding to C–H stretching, N–H<sub>2</sub> groups, and C–O–C stretching, respectively.<sup>35,36</sup>

The functional groups existing in pure CS and NEG were differentiated by comparing their FTIR spectra (Figure 3C and D). The FTIR spectrum of the NEG (Figure 3D) shows that the major peaks of CS are located around  $3368\text{ cm}^{-1}$  and

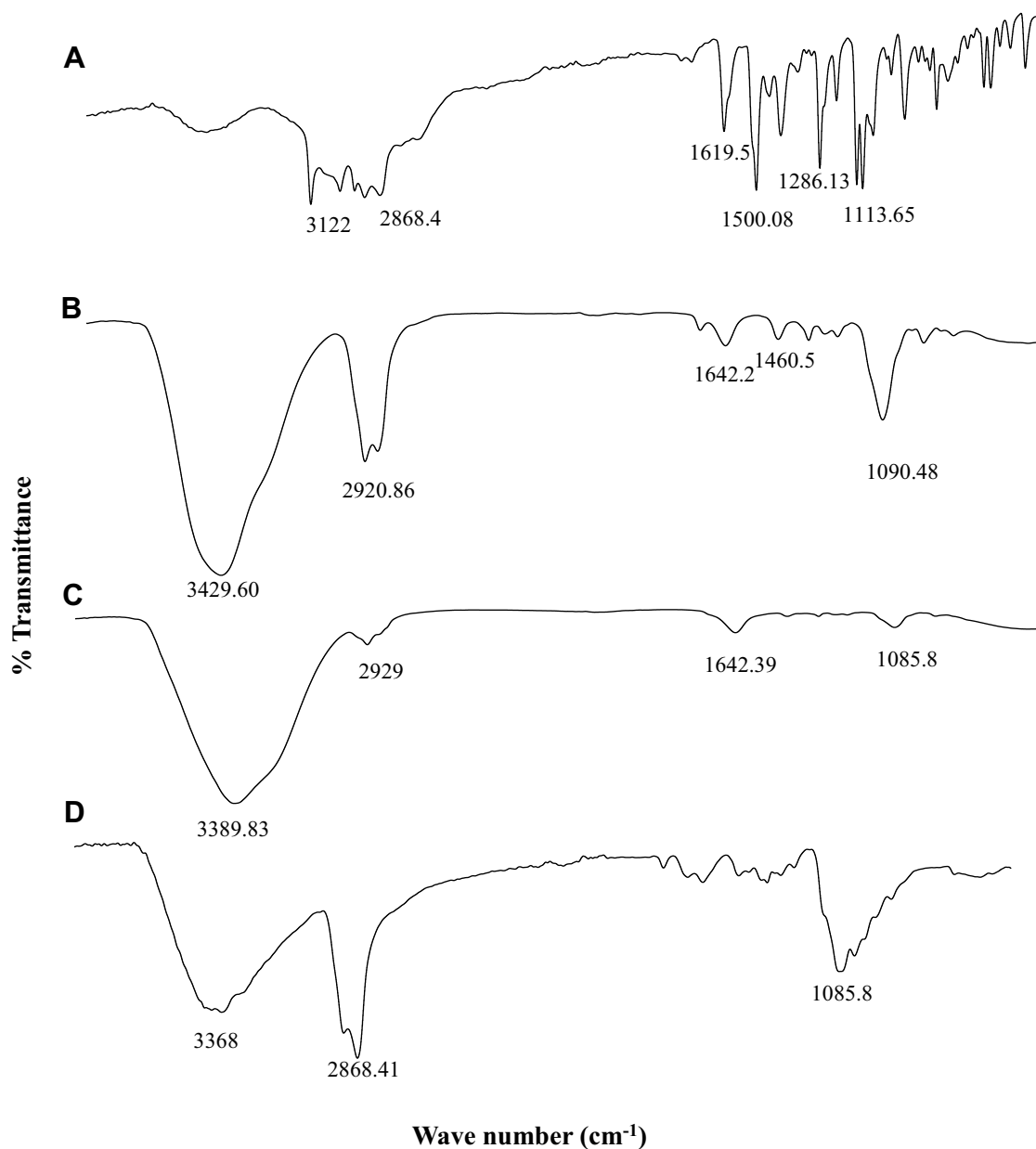


**Figure 3** FTIR spectrum of (A) free Pure 2 drug, (B) blank NE (eucalyptus oil nanoemulsion)/F1, (C) chitosan (CS), and (D) NEG (chitosan-based NEG).

2868.41 cm<sup>-1</sup>, which refer to the stretching vibration of O–H and N–H groups. The peak at 1629 cm<sup>-1</sup> is attributed to the secondary amide C=O bond of the residual acetamido groups. The sharp peak at 1085.8 cm<sup>-1</sup> is a result of O–H deformation of carboxyl groups.<sup>37</sup>

### Drug Content

The uniform distribution of drugs in any pharmaceutical formulation can be confirmed by percent of drug content.<sup>19</sup> Table 5 represents the % drug content in F1

(blank NE), F2 (drug-loaded NE), and F3 (drug-loaded NEG) formulations. As analyzed by HPLC, the drug content in F2 and F3 was insignificantly ( $P > 0.05$ ) different, with 92.34±1.87% and 90.29±1.73%, respectively. The results of the drug content revealed that % drug content fitted within the official limit (ie, 100 ±10%) allowed by the United States Pharmacopeia (USP). The HPLC chromatograms of Pure 2 in F2 and F3 have been given in [Supplementary Figures S3](#) and [S4](#), respectively.

**Table 4** Droplet Size, Zeta Potential, and PDI of F1, F2, and F3 Formulations

Formulations	Droplet Size $\pm$ SD (nm)	Zeta Potential $\pm$ SD (mV)	PDI Ratio
F1	55.87 $\pm$ 0.2	-23.3	0.135
F2	70.84 $\pm$ 0.3	-20.3	0.120
F3	83.74 $\pm$ 1.33	27.9	0.340

Notes: F1, blank emulsion; F2, compound-loaded NE; F3, NEG.

**Table 5** Percent Drug in F2 and F3

Formulations	Drug Required ( $\mu$ g)	Drug Obtained ( $\mu$ g $\pm$ SD)	% Drug Content $\pm$ SD
F1	—	—	—
F2	100	92.34 $\pm$ 1.87	92.34 $\pm$ 1.87
F3	100	90.29 $\pm$ 1.73	90.29 $\pm$ 1.73

## Viscosity

Viscosity plays an important role in the delivery of drugs used via topical or transdermal application. Several characteristics of formulations including the stability, spreadability, drug release, and ease of application are dependent on the viscosity.<sup>15,19,34</sup> The viscosity of the formulations may also be influenced by various polymers used as gelling agents (eg, CS), surfactants and co-surfactants, and different oils and co-solvents used in the formulations.<sup>38</sup> The viscosities of Pure 2-loaded NE (F2) and Pure 2-loaded NEG (F3) formulations, determined at different times and temperatures, are given in Tables 6 and 7, respectively. The viscosity of F3 was significantly higher as compared to F2. This is most likely due to the addition of CS (as gelling agent) to F3. Indeed, according to the study of Kumar et al, the viscosity of any formulation is enhanced by the addition of gelling polymeric agent.<sup>32</sup>

**Table 6** Viscosities (Centipoise) of F2 at the Indicated Temperature and Time

Time	Viscosities at 8°C	Viscosities at 25°C	Viscosities at 40°C
Day 0	6837	6837	6837
Day 1	6830 $\pm$ 13.7	6820 $\pm$ 13.1	5800 $\pm$ 11.2
Day 2	6828 $\pm$ 12.5	6810 $\pm$ 13.3	5800 $\pm$ 12.3
Day 7	6828 $\pm$ 13.2	6808 $\pm$ 13.7	5790 $\pm$ 12.3
Day 14	6827 $\pm$ 13.9	5998 $\pm$ 12.2	5780 $\pm$ 11.6
Day 28	6825 $\pm$ 12.4	5990 $\pm$ 13.2	5550 $\pm$ 13.3

Notes: All the values are calculated as mean $\pm$ SD. F2, Pure 2 compound-loaded NE.

**Table 7** Viscosities (Centipoise) of F3 at the Indicated Temperature and Time

Time	Viscosities at 8°C	Viscosities at 25°C	Viscosities at 40°C
Day 0	12,390	12,390	12,390
Day 1	12,380 $\pm$ 13.7	12,310 $\pm$ 13.1	11,101 $\pm$ 10.2
Day 2	12,380 $\pm$ 12.5	12,200 $\pm$ 13.3	10,990 $\pm$ 11.3
Day 7	12,350 $\pm$ 13.2	12,120 $\pm$ 13.7	10,000 $\pm$ 11.3
Day 14	12,342 $\pm$ 13.9	12,100 $\pm$ 12.2	9950 $\pm$ 11.5
Day 28	12,337 $\pm$ 12.4	11,980 $\pm$ 13.2	9970 $\pm$ 13.2

Notes: All the values are calculated as mean $\pm$ SD; F3, Pure 2 compound-loaded NEG.

## Spreadability of NEG

The extent to which a topically applied pharmaceutical preparation is spread on skin is termed its spreadability. Spreadability is the fundamental feature of topical formulations upon which the therapeutic efficacy is dependent.<sup>19</sup> A small shear is required for a formulation to come out of a container having an optimum spreadability.<sup>39</sup> Various factors, including low and high temperatures, affect the spreadability coefficient of a topical formulation. Indeed, at low temperatures, the viscosity of formulations increased resulting in decreased spreadability. Conversely, at high temperatures, the viscosity of topical formulations decreased, resulting in high spreadability.<sup>19,23</sup> Average spreadability values for blank NE (F1), Pure 2 compound-loaded NE (F2), and Pure 2 compound-loaded NEG (F3) have been presented in Table 8. The formulations kept at high temperatures showed elevated spreadability as compared to the same formulations kept at low temperatures. Moreover, F1 and F2 showed significantly higher spreadability as compared to F3, which can be explained by the absence of the gelling agent CS. There was insignificant difference ( $P>0.05$ ) between F1 and F2.

**Table 8** Average Spreadability Values of F1, F2, and F3 Kept at the Indicated Temperature

Formulations	Spreadability at 8°C	Spreadability at 25°C	Spreadability at 40°C
F1	16.90 $\pm$ 1.11	20.72 $\pm$ 1.35	26.43 $\pm$ 1.98
F2	16.89 $\pm$ 1.17	20.77 $\pm$ 1.10	26.00 $\pm$ 11.2
F3	12.12 $\pm$ 1.10	14.73 $\pm$ 1.30	16.21 $\pm$ 1.13

Notes: All the values are calculated as mean $\pm$ SD. F1, NE; F2, Pure 2 compound-loaded NE; F3, Pure 2 compound-loaded NEG.

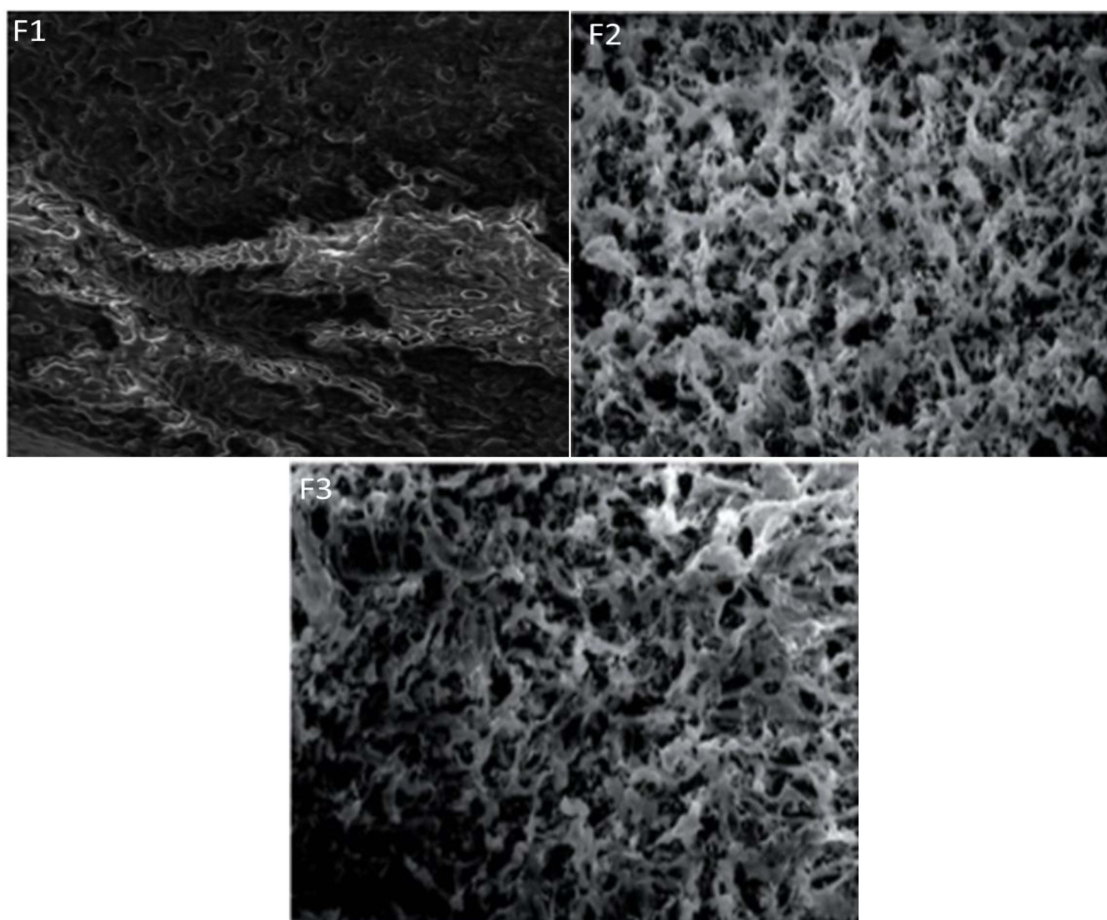


**Figure 4** The SEM images of NE (F1), Pure 2 compound-loaded NE (F2), and chitosan-based nanoemulsion gel (F3).

## Morphological Aspects of the Prepared Nanoemulsions

The morphologies and shapes of the blank NE (F1), Pure 2-loaded NE (F2), and Pure 2-loaded NEG were depicted by SEM as shown in Figure 4. The SEM micrograph of F1 appeared like a mesh, while the SEM micrograph of F2 and F3 showed interconnected pores having random size distribution. The porous structure of the formulations is beneficial giving sufficient space for drug loading. Concordantly, the drug release rate from the formulations and movement of drugs throughout were significantly enhanced.<sup>21,24</sup>

## Pharmacological Analysis of the Prepared Nanoemulsions

### In vitro Drug Release

The therapeutic efficacy of any drug depends upon the drug release from pharmaceutical dosage forms.<sup>11,15,22</sup> The drug release from topical formulation is dependent upon several factors including gelling polymeric agents, emulsifying

agents, spreadability, and viscosity.<sup>20,40</sup> The drug release from F2 (Pure 2 compound-loaded NE) and F3 (Pure 2 compound-loaded NEG) formulations are presented in Figure 5. The percent drug release of F2 was observed as 52%, 60%, 68.8%, 75.5%, 76.11%, and 85.33% at 1 h, 2 hrs, 4 hrs, 6 hrs, 8 hrs, and 12 hours, respectively. Interestingly, the drug release from F3 was comparatively lower than F2 ( $P < 0.03$ ) with 47.2%, 53.8%, 65.2%, 70.29%, 74.33%, and 75.3%. The reduction of drug release from F3, and thus the longer diffusion pathways of drug permeated through the membrane, can be correlated to the presence of the gelling agent CS in F3, which induced a complexity of the gel network.<sup>31</sup> Same results were reported by Yang et al stating that the drug release is inversely proportional to the amount of gelling agent added in the formulation.<sup>16</sup>

### Ex vivo Skin Permeation

Skin permeation is an important feature for efficient transdermal drug delivery.<sup>11</sup> The ex vivo drug permeation studies were conducted for both F2 (Pure 2 compound-loaded NE)

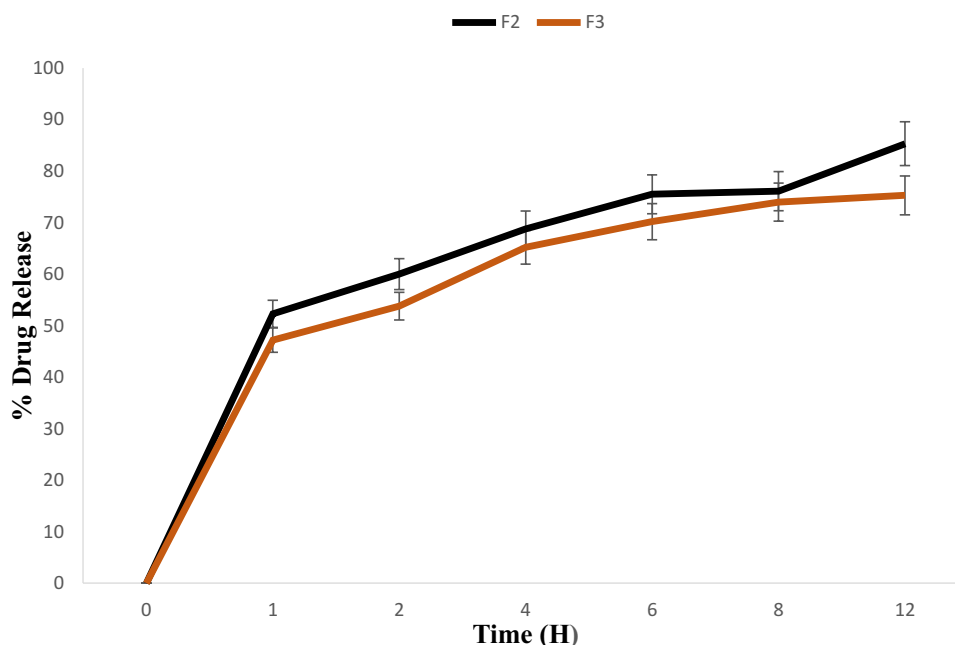


**Figure 5** Drug release (%) of Pure 2 compound-loaded NE (F2) and Pure 2 compound-loaded NEG (F3) formulations at indicated time points.

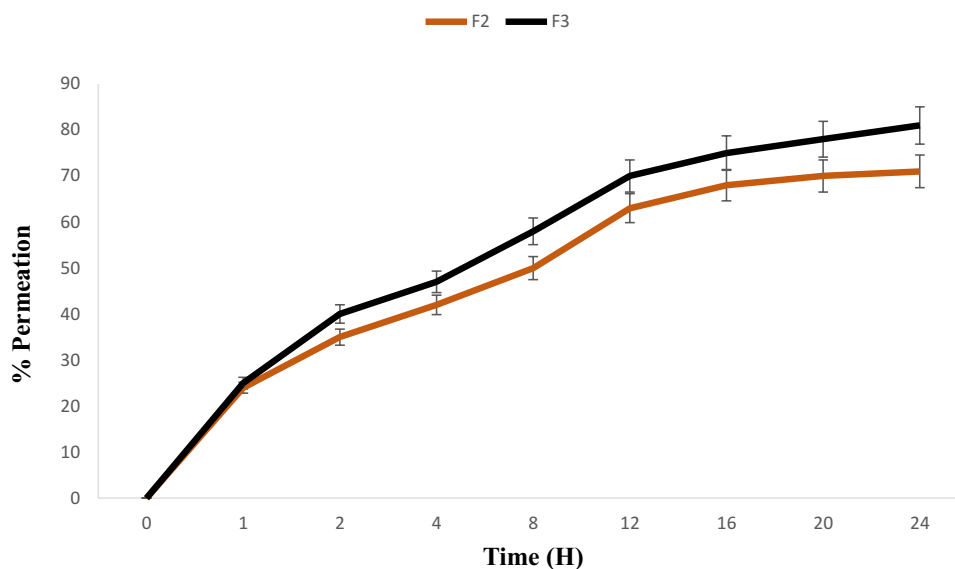


**Figure 6** Permeation (%) of Pure 2 compound-loaded NE (F2) and Pure 2 compound-loaded NEG (F3) formulations at indicated time points.

and F3 (Pure 2 compound-loaded NEG) using rabbit skin. The % drug permeation is given in Figure 6. Drug permeation into the skin is affected by different parameters which include the nature of the drug, particle size (PS), ZP, and surface area.<sup>15,18,19</sup> In the present study, drug permeation was evaluated using Franz diffusion cell. The permeation of F3 (81.80±1.91%) was significantly ( $P<0.05$ ) higher compared to that of F2 (71.15±1.28%). This higher skin permeability of F3 might be attributed to the addition of CS. Indeed, since ZP

of F2 is negative, it induces repelling the from rabbit skin cell membrane which is globally negatively charged because of the phospholipid bilayer.<sup>31</sup> Conversely, due to CS gelation which has a positive ZP (ie, +17.7 mV),<sup>25</sup> F3 was conferred a net positive surface charge (ie, +27.9 mV), which allows F3 to attach to the negatively charged cell membrane, subsequently providing enough time for F3 to penetrate the skin and sneak into the systemic circulation, independently of the larger droplets size of F3 compared to that of F2.

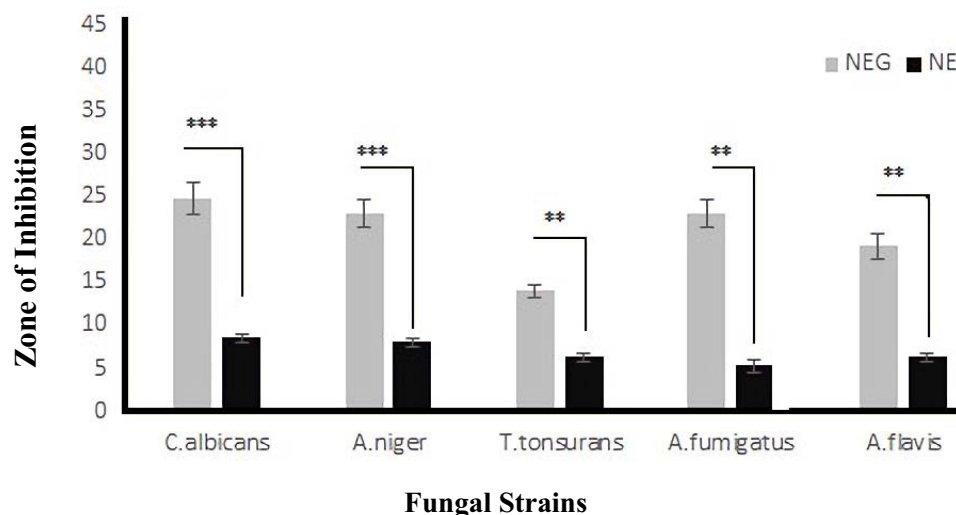


**Figure 7** In-vitro antifungal activity of Pure 2 compound-loaded NE (F2) and Pure 2 compound-loaded NEG (F3) formulations against selected and indicated fungal strains. The data are presented as the mean±SD, and the data were analyzed using ANOVA. \*\* $P < 0.02$  and \*\*\* $P < 0.001$  indicate the statistical significance of antifungal activity of F3 from F2 (used as control).

## Biological Analyses of the Prepared Nanoemulsions

### In vitro Antifungal Assays

Antifungal activity of the Pure 2-loaded NE (F2) and Pure 2-loaded NEG (F3) was assessed using disc-diffusion assay (Figure 7). ZIs of Pure 2 compound-loaded NEG (F3) against *C. albicans*, *A. niger*, *T. tonsurans*, *A. fumigatus*, and *A. flavis* were 23.5±1.1 mm, 21.2±1.6 mm, 13.45±0.99 mm, 19.5±1.4 mm, and 17±1.4mm, respectively (Figure 7). F3 showed significant ( $P < 0.05$ ) antifungal activity against the selected fungal strains, compared to that of Pure 2 compound-loaded NE (F2) (Figure 7). F3 also showed significantly ( $P < 0.05$ ) higher antifungal activity compared to that of the free Pure 2 compound. These observations with F3 can be explained by the presence of CS, which displays inherent antifungal activity and thus may have a synergistic effect with the entrapped drug.<sup>35</sup> Several studies have reported the antifungal activity of CS against *Aspergillus* species, *Candida* species, and *Rhizopus* species.<sup>25,33,38</sup> The antifungal activity of CS may be attributed to its polycationic nature, enabling interactions with the negatively charged phospholipids present in the membrane of fungi. This interaction causes high permeability of the fungal membrane, leading to leaking of the fungal cellular content and subsequent cell death.<sup>37,41</sup> This could not be the case with F2 which has negative ZP, causing repulsive effect against the fungal membrane.

Further, an antifungal activity of empty/blank NE (F1) has been noticed, which may be attributed to the eucalyptus

oil used in the formulation. According to Alam et al, the eucalyptus oil exerts a wide spectrum of biological activity including antifungal, antibacterial, nematicidal, and acaricidal.<sup>40</sup> Thus, both eucalyptus oil and CS conferred a synergistic of additive effect to the antifungal drug effect.

### In vivo Antifungal Assay

Microbial secondary metabolites and their active compounds have been extensively studied for antifungal and antibacterial activities.<sup>1,2,17</sup> However, to date, the antifungal activities of *Pseudomonas fluorescens*-derived metabolites are seldom reported. Therefore, the anti-fungal activity of the nanoemulsified Pure 2 compound was evaluated after significant induction of candidiasis (*Candida* infection) in rabbits (Figure 8). F2 (Pure 2-loaded NE) and F3 (Pure 2-loaded NEG) exhibited potent antifungal activities in vitro. Blank NEG was used as internal control, while the standard marketed cream clotrimazole/Canesten<sup>®</sup> was used as external control.

The blank NEG-treated animals were found to have bleeding after eight days, while healing of lesions and wounds was observed on 4<sup>th</sup> day in groups treated either with Pure 2-loaded NEG or marketed antifungal cream. There was insignificant difference ( $P > 0.05$ ) between the standard group and the experimental group of animals, while both groups significantly differed ( $P < 0.05$ ) with the control group of animals. Complete recovery from the infection was achieved on day 8 with Pure 2-loaded NEG or marketed antifungal cream, whereas animals treated with blank NEG-treated animals did not recover until day 12.

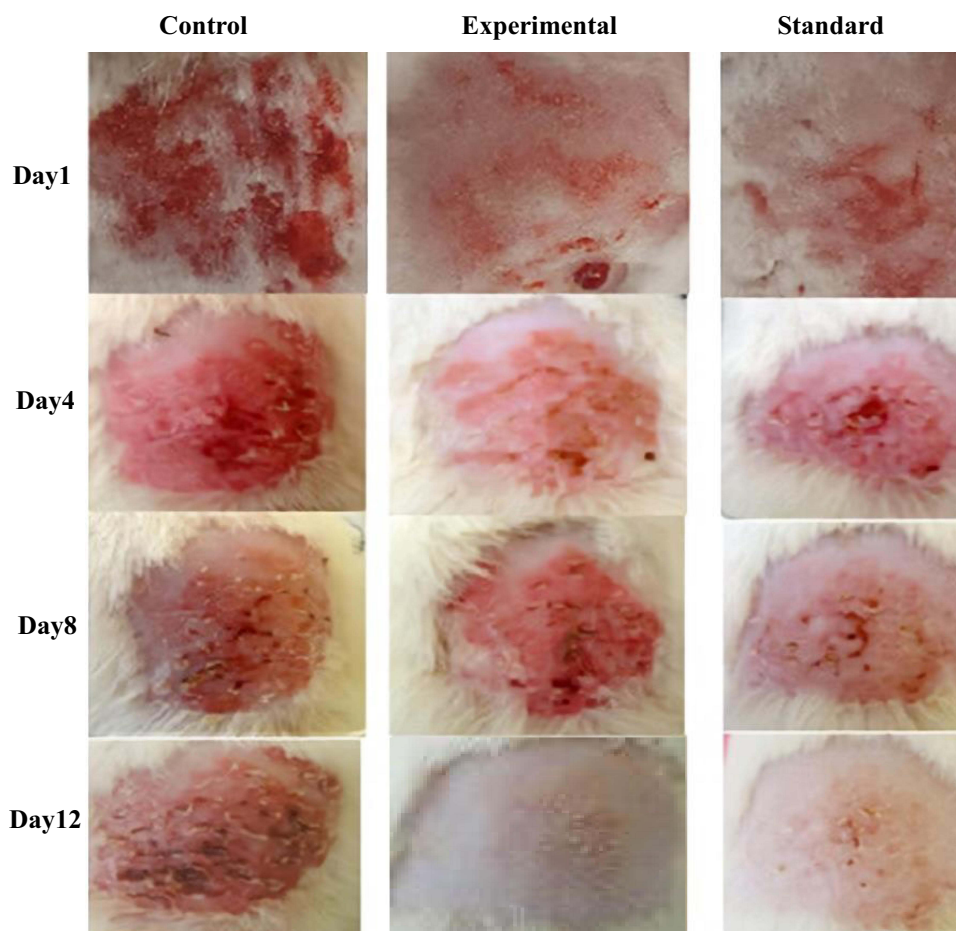


**Figure 8** In vivo time-course of topical antifungal activity of control (blank NEG), experimental (Pure 2-loaded NEG), and standard cream (clotrimazole/Canesten®) in rabbits. The time is indicated.

The recovery from fungal infections is possible only if (i) a large amount of drug releases from the dosage form, (ii) permeates into the skin layers, and (iii) the drug/compound is retained at the infection site for a long period of time.<sup>6,15,39</sup> Moreover, the killing of fungus may be attributed to the smaller globule size, allowing high permeation and subsequently creating a drug depot under stratum corneum of the skin.<sup>26</sup> Hence, Pure 2-loaded NEG elicited a potential therapeutic effect and could be considered as a possible alternative for the effective treatment of *Candida* infections to current and conventional therapeutic drugs (eg, clotrimazole).

## Conclusion

Bacterial isolates from the red soil samples have the potential to act as a new natural source for novel antimicrobial agents against several pathogenic fungal strains. The secondary metabolites produced by *Pseudomonas fluorescens* may have advantages in terms of efficiency,

safety, and cost-effectiveness for high-scale production. The optimized formulation showed droplet size in nanoscale and uniform distribution. The formulation was evaluated for 28 days under exaggerated conditions and found physically and thermodynamically stable. There was slight change in pH values; however, these were in the acceptable range. The drug content, viscosity, and spreadability were within official pharmacopeia limits. The drug release and drug permeation were optimum. Herein, the in vitro and in vivo antifungal studies revealed that optimized NEG can be used to successfully entrap the isolated Pure 2-derived *fluorescens* compound, which was found potent and safe for the topical treatment of invasive fungal infections. Hence, nanoemulsions prepared with natural and biocompatible compounds (eucalyptus oil, chitosan, Pure 2) can represent a very promising therapeutic strategy and option to overcome fungal MDR to the current conventional available therapies.

## Abbreviations

CS, chitosan; MFC, minimum fungicidal concentration; NE, nanoemulsion; NEG, nanoemulsion gel; PAE, phthalic acid ester; PBS, phosphate buffer solution; PS, particle size; SEM, scanning electron microscopy; ZP, zeta potential; ZI, zone of inhibition.

## Data Sharing Statement

Data available upon request to the authors.

## Acknowledgments

The Deanship of Scientific Research (DSR) at King Abdulaziz University, Jeddah, Saudi Arabia has funded this project, under grant no. (RG-28-166-42). The authors, therefore, acknowledge with thanks DSR technical and financial support. The authors would also like to thank Higher Education Commission (HEC) of Pakistan for approving NRPDU.

## Disclosure

Farid Menaa is employed by the California Innovations Corporation, San Diego, CA, 92037, USA. The authors declare no other potential conflicts of interest for this work nor in submission of this manuscript.

## References

- Uzair B, Menaa F, Khan BA, et al. Isolation, purification, structural elucidation and antimicrobial activities of kocumarin, a novel antibiotic isolated from actinobacterium *Kocuria marina* CMG S2 associated with the brown seaweed *Pelvetia canaliculata*. *Microbiol Res*. 2018;206: 186–197.
- Bushra U, Firdous N, Khan BA, Fatima S, Kausar S, Bano R. Isolation and characterization of antibiotic producing bacterial strains from red soil of Himalayan region of Pakistan. *Pak J Pharm Sci*. 2017;30:2393–2397.
- Zhang X, Song J, Klymov A, et al. Monitoring local delivery of vancomycin from gelatin nanospheres in zebrafish larvae. *Int J Nanomed*. 2018;13:53–77.
- Uzair B, Ahmed N, Ahmad VU, Kousar F. A new antibacterial compound produced by an indigenous marine bacteria—fermentation, isolation, and biological activity. *Nat Prod Res*. 2016;20:1326–1331.
- Felic H, Gong H, Qi Y. In vitro and in vivo antifungal activities and mechanism of heteropolytungstates against *Candida* species. *Sci Rep*. 2017;7:16942.
- Verma S, Bhardwaj A, Vij M, Bajpai P, Goutam N, Kumar L. Oleic acid vesicles: a new approach for topical delivery of antifungal agent. *Artif Cells Nanomed Biotechnol*. 2019;42:95–101.
- Zhang L. Pharmacokinetics and drug delivery systems for puerarin, a bioactive flavone from traditional Chinese medicine. *Drug Deliv*. 2019;26:860–869.
- Durand GA, Raoult D, Dubourg G. Antibiotic discovery: history, methods and perspectives. *Int J Antimicrob Agents*. 2019;53: 371–382.
- Gámez E, Mendoza G, Salido S, Arruebo M, Irusta S. Antimicrobial electrospun polycaprolactone-based wound dressings: an in vitro study about the importance of the direct contact to elicit bactericidal activity. *Advan Wound Care*. 2019;8:438–451.
- Li H, Gong H, Qi Y. In vitro and in vivo antifungal activities and mechanism of heteropolytungstates against *Candida* species. *Sci Rep*. 2019;7:16942.
- Khan AB, Yasmin A, Tariq HK, Mughal Q, Sultan MA, Muhammad KK. Novel insight into potential leishmanicidal activities of transdermal patches of *nigella sativa*: formulation development, physical characterizations, and in vitro/in vivo assays. *Assay Drug Develop Technol*. 2021;3:2335–2341.
- Hosny KM, Sindi AM, Alkhalidi HM, et al. Oral gel loaded with penciclovir–lavender oil nanoemulsion to enhance bioavailability and alleviate pain associated with herpes labialis. *Drug Deliv*. 2021;28 (1):1043–1054.
- Hosny KM, Sindi AM, Alkhalidi HM, et al. Development of omega-3 loxoprofen-loaded nanoemulsion to limit the side effect associated with NSAIDs in treatment of tooth pain. *Drug Deliv*. 2021;28 (1):741–751.
- Yen CC, Chen YC, Wu MT, Wang CC, Wu YT. Nanoemulsion as a strategy for improving the oral bioavailability and anti-inflammatory activity of andrographolide. *Int J Nanomed*. 2019;13:669.
- Afzal H, Abdus SK, Singh MN, et al. Nanoemulsion gel-based topical delivery of an antifungal drug: invitro activity and invivo evaluation. *Drug Deliv*. 2016;23:642–657.
- Yang M, Gu Y, Yang D, Tang X, Liu J. Development of triptolide-nanoemulsion gels for percutaneous administration: physicochemical, transport, pharmacokinetic and pharmacodynamic characteristics. *J Nanobiotech*. 2017;15:88.
- Shah IN, Panpan Z, Hongjie S, et al. Two new isochromane derivatives penisochromanes A and B from ascidian-derived fungus *Penicillium* sp. 4829. *Nat Prod Res*. 2019;33:1262–1268.
- Liuhon Z, Shah IN, Dilfaraz K. Induction of diverse bioactive secondary metabolites from the mangrove endophytic fungus *trichoderma* sp. (Strain 307) by Co-cultivation with *Acinetobacter johnsonii* (Strain B2). *Mar Drugs*. 2017;35: 1–14.
- Burki IK, Khan MK, Khan BA, Uzair B, Braga VA, Jamil QA. Formulation development, characterization, and evaluation of a novel dexibuprofen-capsaicin skin emulgel with improved in vivo anti-inflammatory and analgesic effects. *AAPS PharmSciTech*. 2020;21:211–220.
- Huang L, Zhu X, Zhou S, et al. Phthalic acid esters: natural sources and biological activities. *Toxins*. 2021;13:495.
- Valizadeh A, Shirzad M, Pourmand MR, Farahmandfar M, Sereshti H, Amani A. Levofloxacin nanoemulsion gel has a powerful healing effect on infected wound in streptozotocin-induced diabetic rats. *Drug Deliv Trans Res*. 2021;11:292–304.
- Khan BA, Khan A, Khan MK, Braga VA. Preparation and properties of high sheared Poly(Vinyl Alcohol)/Chitosan blended Hydrogels films with *Lawsonia inermis* extract as wound dressing. *J Drug Deliv Sci Technol*. 2020;61:456–462.
- Hosny KM, Aldawsari HM, Bahmdan RH, et al. Preparation, optimization, and evaluation of hyaluronic acid-based hydrogel loaded with miconazole self-nanoemulsion for the treatment of oral thrush. *AAPS PharmSciTech*. 2019;20:297. doi:10.1208/s12249-019-1496-7
- Eid A, Hesham A, Enshasy E, Ramlan A, Nagib A, Elmarzugiet H. Preparation, characterization and anti-inflammatory activity of swieteniamacrophylla nanoemulgel. *J Nanomed Nanotechnol*. 2014;5: 23–29.
- Irshad U, Shefaat US, Khan MK, Kifayat US, Khan BA. Chitosan (Poly-(D) glucosamine) based solid lipid nanoparticles of dexibuprofen for topical delivery: formulation development and characterizations. *Main Group Chem*. 2021;37:34–40.
- Isnan A, Kamei Y. Bioactive substances produced by marine isolates of *Pseudomonas*. *J Ind Microbiol Biotechnol*. 2009;36:1239–1248.
- Mandryk MN, Kolomiet EL, Dev ES. Characterization of antimicrobial compounds produced by *Pseudomonas aurantiaca* S-1. *Polish J Microbiol*. 2007;56:245–250.



28. Scales BS, Dickson RP, LiPuma JJ, Huffnagle GB. Microbiology, genomics, and clinical significance of the *Pseudomonas fluorescens* species complex, an unappreciated colonizer of humans. *Clin Microbiol Rev*. 2014;27:927–948.
29. Sari TP, Mann B, Kumar R, et al. Preparation and characterization of nanoemulsion encapsulating curcumin. *Food Hydrocoll*. 2015;43: 540–546.
30. Martinez LD, Martinez A, Vazquez ER, Cerbon M. The impact of Di-(2-ethylhexyl) Phthalate and Mono(2-ethylhexyl) Phthalate in placental development, function, and pathophysiology. *Environ Int*. 2021;146:106–125.
31. Asadinezhad S, Khodaiyan F, Salami M, Hosseini H, Ghanbarzadeh B. Effect of different parameters on Orange oil nanoemulsion particle size: combination of low energy and high energy methods. *J Food Measur Charac*. 2019;13: 2501–2509.
32. Kumar N, Mandal A. Surfactant stabilized oil-in-water nanoemulsion: stability, interfacial tension, and rheology study for enhanced oil recovery application. *Ener Fuels*. 2018;32:6452–6466.
33. Sharif B, Torabi S, Azarpanah A. Optimization of ibuprofen delivery through rat skin from traditional and novel nanoemulsion formulations. *Iranian J Pharm Res*. 2012;11:47–58.
34. Eid A, Elmarzugi NA, El-Enshasy HA, Arafat OM. A novel Swieteniamacrophylla oil self-nanoemulsifying system: development and evaluation. *Int J Pharm Pharm Sci*. 2013;5: 639–644.
35. Bharathi D, Ranjithkumar R, Chandarshekar B, Bhuvaneshwari V. Preparation of chitosan coated zinc oxide nanocomposite for enhanced antibacterial and photocatalytic activity. *Int J Biol Macromol*. 2019;129:989–996.
36. Pant M, Dubey S, Patanjali PK, Naik NS, Sharma S. Insecticidal activity of eucalyptus oil nanoemulsion with karanja and jatropa aqueous filtrates. *Int J Biodeter Biodegrad*. 2014;91:119–127.
37. Basit HM, Cairul M, Mohd I, et al. Formulation and evaluation of microwave-modified chitosan-curcumin nanoparticles —a promising applications following burn wounds. *Polym*. 2020;12:1–20.
38. Bagheri H, Ghasemi F, Barreto GE, Rafiee R, Sathyapalan T, Sahebkar A. Effects of curcumin on mitochondria in neurodegenerative diseases. *BioFactors*. 2020;46:5–20.
39. Rady MH, Mo S, Salama M. Eucalyptus oil nano-emulsion encapsulated in chitosan beads as a new approach in control of *Culex pipiens* larvae. *Int J Mosquito Res*. 2019;6:63–69.
40. Alam P, Shakeel F, Anwer K, Foudah AI, Alqarni MH. Wound healing study of eucalyptus essential oil containing nanoemulsion in rat model. *J Oleo Sci*. 2018;21:1–12.
41. Abdullah A, Khan MK, Khan BA. Preparation, characterizations and evaluation of antifungal activity of eugenol-linalool emulgel against anthropophilic dermatophytic trichophyton rubrum. *Main Group Chem*. 2021;37 1–15.

## International Journal of Nanomedicine

Dovepress

## Publish your work in this journal

The International Journal of Nanomedicine is an international, peer-reviewed journal focusing on the application of nanotechnology in diagnostics, therapeutics, and drug delivery systems throughout the biomedical field. This journal is indexed on PubMed Central, MedLine, CAS, SciSearch®, Current Contents®/Clinical Medicine,

Journal Citation Reports/Science Edition, EMBase, Scopus and the Elsevier Bibliographic databases. The manuscript management system is completely online and includes a very quick and fair peer-review system, which is all easy to use. Visit <http://www.dovepress.com/testimonials.php> to read real quotes from published authors.

Submit your manuscript here: <https://www.dovepress.com/international-journal-of-nanomedicine-journal>